Desalination and Water Treatment
www.deswater.com

doi:10.5004/dwt.2019.23953

148 (2019) 259–269
April

Removal of Cu and Cr ions from aqueous solutions by a chitosan based flocculant

Yongjun Sun[a,*], Aowen Chen[a], Wenquan Sun[a], Kinjal J. Shah[b], Huaili Zheng[c], Chengyu Zhu[a]

[a]*College of Urban Construction, Nanjing Tech University, Nanjing, 211800, China, email: sunyongjun@njtech.edu.cn (Y. Sun), 1064442347@qq.com (A. Chen), coneflower@163.com (W. Sun), 2506885738@qq.com (C. Zhu)*
[b]*Graduate Institute of Environmental Engineering, National Taiwan University, 71 Chou-Shan Road, Taipei City, 10673, Taiwan, email: kinjalshah8@gmail.com (K.J. Shah)*
[c]*Key laboratory of the Three Gorges Reservoir Region's Eco-Environment, State Ministry of Education, Chongqing University, Chongqing, 400045, China, email: zhl@cqu.edu.cn (H. Zheng)*

Received 6 October 2018; Accepted 14 February 2019

ABSTRACT

In this work, carboxylated chitosan and acrylamide are used to synthesize a graft-modified natural polymer flocculant carboxylated chitosan-graft-acrylamide (CCSPAM) by UV-induced polymerization for copper and chromium removal. The effects of total monomer concentration, monomer mass ratio, pH value, photoinitiator concentration, and illumination time on the synthesis performance of CCSPAM were investigated regarding intrinsic viscosity (IV), grafting rate (GR), and grafting efficiency (GE). Various analytical techniques characterize the physicochemical characteristics of CCSPAM. Single factor experiments are used to investigate the effect of dosage, pH value, and reaction time on the chelation and capture of heavy metal ions by CCSPAM. The results show that the optimal IV, GR, and GE of CCSPAM achieved at total monomer concentration 30%, monomer mass ratio 1:4, pH 7.0, photoinitiator concentration 0.03%, and irradiation time 2 h are 1412.2 mL/g, 394.1%, and 84.1%, respectively. The experimental data of flocculation show that CCSPAM has a good total Cu and total Cr removal efficiency of 74.8% and 70.6% at dosage 2.0 mg/L, pH 6.0, and reaction time 2h, respectively. Fom the investigation, it is concluded that the grafted chitosan (CCSPAM) could be a be an effective and eco-friendly flocculant for removal of total Cu and total Cr ions from aqueous system.

Keywords: Carboxylated chitosan; Flocculant; Heavy metal removal; Flocculation; Chelation

1. Introduction

With the rapid development of industrialization in manufacturing, mining, electroplating, rubber, and other industries, a significant amount of heavy metal wastewater is discharged into the natural environment [1–3]. Heavy metal ion pollution of water has become a focus of social concern [4,5]. Since heavy metals are non-biodegradable and they tend to accumulate in the living body through the food chain, they have seriously threatened the physical health of humans and the proper functioning of ecosystems [6]. Heavy metal ions such as zinc, cadmium, copper, lead, platinum, etc. are toxic or carcinogenic. When excessive levels of copper ions are accumulated in the human body, it can cause diarrhea, muscle cramps, and even coma [7]. Lead is prone to accumulate in the body and causes nerves, hematopoietic and digestive disorders [8]. Therefore, how to achieve a harmless treatment of waste water containing heavy metals has become a global problem [9].

Because heavy metals such as Hg, Pb, Cu, Cd, and Ni have non-degradable characteristics, their removal can only be achieved by changing their existing modes and transformation forms [10]. Current conventional methods of treatment mainly include membrane separation, chemical precipitation, electrolysis, ion exchange, activated carbon, and biosorption [11]. However, these methods have few deficiencies, for example, the chemical precipitation method produces a significant amount of sludge; the mem-

*Corresponding author.

brane separation method has a high cost and complicated process in the water treatment process; and due to the rapid saturation adsorption of the resin, the ion exchange method is not suitable for high concentration heavy metal ion wastewater [12,13]. In recent years, flocculation has been widely used as a highly efficient, economical, and convenient method for removing heavy metals [14,15]. However, in most cases, inorganic or organic synthetic polymer flocculants used for removing heavy metal ions by flocculation are deficient in environmental friendliness and challenging to be degraded by microorganisms [16]. Therefore, naturally modified polymer flocculants that are characterized by low cost, non-toxicity, and biodegradability have attracted more attention [17]. Due to the existence of macromolecular structure surface active groups (hydroxyl, amino or acetylamino functional groups), such natural macromolecule polymers are enabled to achieve the removal of heavy metals by flocculation and chelation.

At the same time, as a class of natural macromolecules with amino and hydroxyl groups, chitosan can form stable complexes with dissolved heavy metal ions due to its extraordinarily active and adjacent units [18]. However, chitosan is relatively hydrophobic and can only dissolve in weakly acidic environments, which limits its use in the removal of heavy metal ions in aqueous solutions [19]. To improve the hydrophilic properties of chitosan and increase its chelation and trapping ability for heavy metal ions, chitosan is modified by graft copolymerization to obtain a natural, modified macromolecular flocculant that was used to remove copper [20].

In this study, a naturally modified flocculant CCSPAM is prepared by UV-initiated polymerization and applied in the flocculation tests to remove Cu(II) and Cr(III). The microstructure of CCSPAM is characterized by scanning electron microscopy (SEM), Fourier transforms infrared spectroscopy (FTIR), X-ray diffraction (XRD), thermogravimetry-differential thermal analysis (TG-DTG), and nuclear magnetic resonance spectroscopy (^{1}H NMR). The effects of dosing amount, pH value, and reaction time on the chelation and capture of heavy metal ions by CCSPAM are investigated in detail.

2. Experimental

2.1. Materials

Carboxylated chitosan (CCS, CAS: 9012-76-4) and acrylamide (AM) are of analytical grade and purchased from Shanghai Aladdin Bio-Chem Technology Co. LTD (China). Copper sulfate ($CuSO_4{\cdot}5H_2O$) and potassium dichromate ($K_2Cr_2O_7$) are sourced from Nanjing Shengjianquan instrumental glass Co. LTD (China), and all the other reagents used in the experiments are used as received without further purification.

2.2. Synthetic and characterizations of CCSPAM

The possible scheme of synthesizing CCSPAM is shown in Fig. S1. A certain amount of 3.0 g CCS, 7.0 g AM, and 35.0 mL distilled water are weighed in a wide-mouth quartz bottle according to mass ratio by experiment optimization process, and stirring the mixture until it is completely dissolved. H_2SO_4 and NaOH solution is used to adjust pH value, and the reactor is degassed with nitrogen for 20 min to remove oxygen, followed by addition of photoinitiator V50 at a certain mass ratio, and then followed by pouring nitrogen gas for 10 min and sealed. The sealed quartz bottle is placed in a UV reactor; the reaction is carried out for 30~60 min. The quartz bottle is taken out of the reactor and allowed to stand for aging for 1 h to obtain a colorless translucent polymer colloid CCSPAM. The graft copolymer colloid product was sheared into particles with particle diameter of 1–3 mm, and immersed in an ethanol and acetone solution with a volume ratio of 1:1 to remove unreacted monomers and small molecule polymers. The purified CCSPAM was dried in a vacuum oven to obtain a solid CCSPAM, and finally the solid CCSPAM was ground and passed through a 200 mesh screen to obtain a CCSPAM powder. The obtained CCSPAM sample powder is characterized by infrared spectroscopy (IR), nuclear magnetic resonance spectroscopy (^{1}H NMR), thermogravimetric analysis (TG-DTG), and scanning electron microscope (SEM).

2.3. Flocculation test and analytical method

Copper sulfate ($CuSO_4{\cdot}5H_2O$) and potassium dichromate ($K_2Cr_2O_7$) is used to prepare a heavy metal simulated wastewater with a certain concentration of 20.0 mg/L Cu^{2+} and 20.0 mg/LCr^{6+}, respectively. The experiments are conducted on a six-link coagulation test mixer (ZR4-6, Shenzhen Zhongrun Water Industrial Technology Development Co., Ltd.). A predetermined amount of flocculants are added into copper or chromium wastewater according to the experiment design, and the programmed paddle mixer is set at 350 rpm for 3 min to ensure sufficiently mixing flocculants with wastewater. After the rapid mixing, the copper or chromium wastewater is carried out at a slow mixing rate at 60 rpm for time according to the designed reaction time, and finally, settle for 15 min as a sedimentation time. Experiments are carried out to control the reaction conditions of flocculation experiments, and the concentration of residual heavy metal ions in the supernatant after flocculation and precipitation is measured using a flame atomic absorption spectrophotometer (GGX-100, Beijing Haiguang Instrument Co., Ltd.).

3. Results and discussion

3.1. Optimization of synthesizing CCSPAM

3.1.1. Effect of total monomer concentration on optimization of synthesizing CCSPAM

Fig. S2 presents the effect of total monomer concentration on intransic viscosity and graft ratio. The IV, GR, and GE of CCSPAM are increased slowly at a total monomer concentration of less than 20%. The maximum value of intrinsic viscosity, grafting ratio, grafting ratio of CCSPAM obtained at total monomer concentration 30% are 1342.35 mL/g, 356.1%, and 89.03%, respectively (See Fig. S2a). When the monomer concentration is higher than 30%, IV, GR, and GE of CCSPAM tend to decrease as the total monomer concentration increases.

When the total monomer concentration is low, the probability of contact collisions between monomer molecules is low, resulting in a low probability of reaction and low IV, GR, and GE of CCSPAM [21].The reaction rate increases as the concentration of carboxylated chitosan and acrylamide in the reaction system increases. Moreover, with the increase of carboxylated chitosan and acrylamide, the system exhibits a highly viscous state, and some raw materials cannot be completely dissolved, and therefore cannot participate in the reaction. Also, if the stirring time is extended, the dissolved chitosan will be partially hydrolyzed with stirring. Thus, a high concentration of monomer concentration is not conducive to the progress of the reaction, resulting in reducing the final product of IV, GR, and GE [22].The amino group of chitosan generates free radicals under the action of ultraviolet light, and the C=C double bond of acrylamide absorbs ultraviolet light energy to undergo graft copolymerization reaction with the amino group of chitosan. And then chitosan is grafted with acrylamide to produce graft copolymer CCSPAM. In summary, the optimal total monomer concentration of 30% was considered as the optimum concentration for further synthesis.

3.1.2. Effect of monomer ratio on optimization of synthesizing CCSPAM

Fig. S3 presents the effect of monomer ratio on intransic viscosity and graft ratio. When the mass ratio of the monomer is less than 1:2, the intrinsic viscosity of CCSPAM decreases with the increase of monomer mass ratio (See Fig. S3a).When the mass ratio of the monomer is higher than 1:2, the intrinsic viscosity of CCSPAM first rises and then decreases with the increase of monomer mass ratio, and reaches the maximum value of 1456.73 mL/g at the monomer mass ratio 1:4. In the case of graft ratio, it increased first and then decreased with the increasing the monomer mass ratio. It reached the maximum value of 525.76% at the mass ratio of monomer 1:3. Comparatively, the grafting efficiency of the final product shows an irregular trend with the increase of the monomer mass ratio, but it reaches the maximum value of grafting efficiency 87.60% at monomer mass ratio 1:4.

The grafting rate of the reaction increased significantly with the decrease of the mass ratio of CCS and AM, and the grafting efficiency begins to decrease rapidly to a certain extent. The addition of acrylamide monomers increases the colliding chance of monomer molecules with the chitosan molecules, facilitating the grafting of monomer molecules onto the chitosan macromolecules. However, the increase of acrylamide also promotes the formation of homopolymer-polyacrylamide, resulting in low utilization of AM. The number of sugar residues in the chitosan molecule has a certain amount to be attached by AM monomers, so the mass ratio of CCS and AM has the optimal value. However, when the amount of AM is too large, the stretching of the two monomer chains can be restrained, leading to decreasing the interaction probability between the monomers. At this time, a large amount of homopolymerization reaction occurs, resulting in reducing the grafting rate and grafting of CCSPAM [22,23]. In summary, the optimal monomer mass ratio of CCS and AM for the synthesis reaction is 1:4.

3.1.3. Effect of pH on optimization of synthesizing CCSPAM

As seen in Fig. S4, the pH value influence the intrinsic viscosity of the final product (CCSPAM). It shows a trend of increasing at first and then decreasing, and again it reaches the maximum value of 1351.16 mL/g at pH = 7.0. The grafting rate and grafting efficiency of the final product shows a rapid trend of increasing first and then decreasing rapidly with the increase of pH value and reached the maximum grafting rate and grafting efficiency of 390.66% and 97.67% at pH = 7.0, respectively.

The pH value has an important influence on the properties of the final product CCSPAM, and the pH value affects the reactivity ratio of each synthetic monomer and the decomposition rate of the photoinitiator. Under strongly acidic conditions, imidization reactions between the amide bonds inside the acrylamide molecular structure are easy to occur, leading to the formation of cross-linked or dendritic polymers with poor solubility [24]. Under alkaline conditions, acrylamide will undergo chain transfer, and the chain transfer rate will increase further, leading to reducing IV, GR, and GE of CCSPAM [25]. In summary, the optimum pH for the synthesis reaction is 7.0.

3.1.4. Effect of photoinitiator concentration on optimization of synthesizing CCSPAM

It can be seen that with the increase of the photoinitiator concentration, the grafting rate and grafting efficiency of CCSPAM first increase rapidly and then decrease gradually (See Fig. S5). When the photoinitiator concentration is less than 0.03%, the intrinsic viscosity of CCSPAM continued to increase. When the photoinitiator concentration was greater than 0.03%, IV, GR, and GE of CCSPAM begin to decrease. As shown in Fig. S5, the optimal IV, GR, and GE of CCSPAM at photoinitiator concentration 0.03% are 1384.2 mL/g, 318.2% and 81.2%, respectively.

When the photoinitiator concentration is less than 0.03%, there are insufficient free radicals generated; the chain initiation reaction is difficult to proceed with a small amount of active center of the reaction system and the slow chain growth [26]. When the total initiator concentration exceeds 0.03%, the excess initiator also causes the reactants to have a low degree of grafting and low molecular weight. The reason is that a large amount of free radicals are generated instantaneously with increasing total concentration of the initiator, resulting in the generation of too many active centers for forming short chain substances in a short time. Moreover, the collision of reactive groups may cause "chain transfer" to hinder the further progress of the reaction [27]. In summary, the optimal photoinitiator concentration for this synthesis reaction is 0.03%.

3.1.5. Effect of illumination time on optimization of synthesizing CCSPAM

The effects of illumination time on intransic viscosity and graft ratio are shown in Fig. S6. As the illumination time increases, IV, GR, and GE of CCSPAM increases first and then decreases gradually. The maximum value of IV, GR, and GE of CCSPAM at illumination time 2 h are 1412.17

mL/g, 394.14%, and 84.13%, respectively. In the process of product polymerization, with the increase of illumination time by the irradiation of ultraviolet light, the breaking rate of the molecular bond accelerated, and the intrinsic viscosity of the product increased [28]. However, with the further extension of the illumination time, the rise of reaction solution temperature can cause cross-linking reaction of monomers. So that the viscosity in the polymerization system rises, and reaction system becomes a colloidal state, leading to reducing the reactivity of the free radicals and carboxylated chitosan [29,30]. In summary, the optimal illumination time for the synthesis of CCSPAM is 2 h.

3.2. Characterization of CCSPAM

3.2.1. SEM characterization

SEM images of (a) CCS and (b) CCSPAM are shown in Fig. S7. The surface morphology of CCS is layered and smooth with some convex areas. The surface of the grafted product CCSPAM became rough and layered after grafting monomer AM. The structure is destroyed and showed a porous structure with a pore diameter of about 0.3–0.8 μm. Compared with CCS, the porous structure of CCSPAM is favorable to increase the specific surface area of the polymer and enhance the adsorption capacity and solubility of the flocculant in aqueous solution, which is conducive to improve the chelation and flocculation performance of CCSPAM on removing heavy metal ions [31].

3.2.2. FTIR spectrum

FTIR spectrums of (a) CCS and (b) CCSPAM are shown in Fig. 1, the absorption peak of CCSPAM at 3489 cm^{-1} is attributed to the –OH, and –NH stretching vibration bands. The absorption peak at 2894 cm^{-1} is attributed to the symmetrical absorption peak of $–CH_2–$ in the AM structural unit. Also, the absorption peak at 1682 cm^{-1} is attributed to the overlap of the stretching vibration peak of the C=O in AM and antisymmetric stretching vibration peak of $–COO^-$, and the absorption peak at 1445 cm^{-1} is attributed to the symmetrical vibrational absorption peak of the carboxyl group. The absorption peak at 1205 cm^{-1} is attributed to the asymmetrical vibrational absorption peaks of C-O-C on the pyran ring of carboxylated chitosan [32]. The characteristic absorption peak of carboxylated chitosan can be observed in FTIR spectrum of CCSPAM. By comparing Figs. 1(a) and (b), it can be seen that a new absorption peak at 2894 cm^{-1} appears in Fig. 1(a) after grafting AM monomer, absorption peaks at 700–1700 cm^{-1} in Fig. 1(a) are similar to those in Fig. 1(b) except for the difference in the peak intensity. This is because new structural units appear in CCSPAM after grafting the AM monomer, indicating that the AM monomer successfully participates in the polymerization [33].

3.2.3. XRD spectrum

XRD patterns of (a) CCS and (b) CCSPAM are shown in Fig. 2, the XRD pattern of carboxylated chitosan contains some smaller impurity peaks in addition to the strong diffraction peak at 2θ= 20°. A broad diffraction peak is observed at 2θ = 21° in the XRD pattern of CCSPAM, and there was sharp diffraction peak observed at =26°. Comparing the XRD patterns of CCS and the graft product CCSPAM, the peak at 2θ = 20° in CCSPAM becomes slow with strong peak intensity, and a new sharp diffraction peak appears at 2θ = 26°. This is due to the introduction of a large number of amine groups that can generate hydrogen bonds after the introduction of AM monomer, which can increase the molecular hydrogen bonding force and effectively destroy the order of the crystal forms [34]. This result indirectly illustrates the success of the photoinitiated graft polymerization of CCS and AM.

3.2.4. TG-DTG curve

TG-DTG curves of (a) CCS and (b) CCSPAM are shown in Fig. 3, and the corresponding thermogravimetric parameters are shown in Table 1. It can be seen from Fig. 3a that there are four stages of weight loss during the range of 40–600°C for CCSPAM. The weight loss temperature range for the first stage was 40–200°C, and the CCSPAM weight loss and the maximum weightless temperature are 4.8% and 111.6°C in this range, respectively, which is caused by

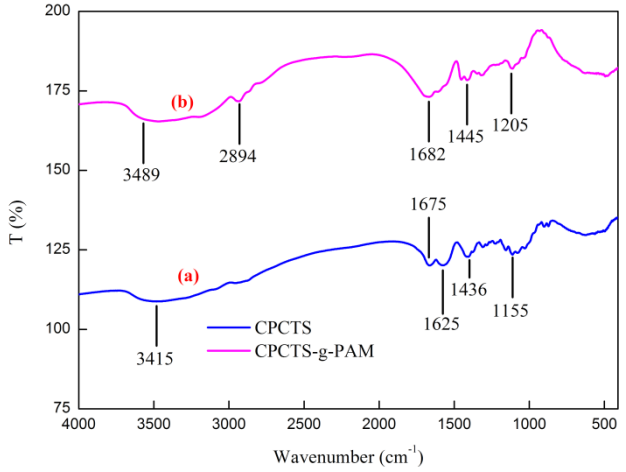

Fig. 1. FTIR spectrums: (a) CCS and (b) CCSPAM.

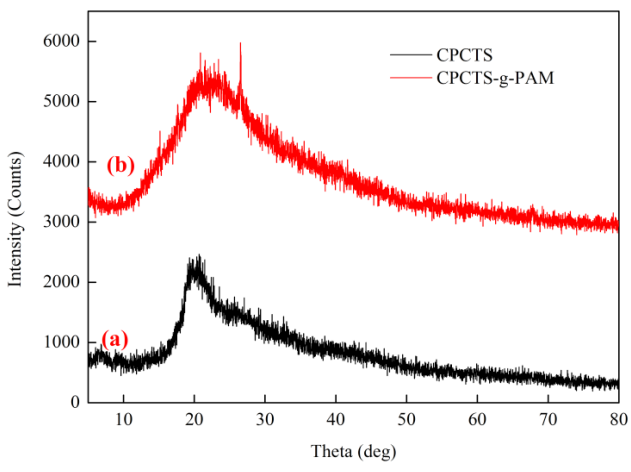

Fig. 2. XRD patterns: (a) CCS and (b) CCSPAM.

the removal of moisture in the sample [35]. The weight loss in the second stage was 200~300°C, the weight loss of the sample in this range and the maximum weightless temperature are 29.7% and 215.6°C, respectively. The weight loss at this stage might be take place by the thermal decomposition of the amide group (-CO-NH-) and the amino group of chitosan [36]. The weight loss in the third stage was in the range of 300–450°C, and the sample weight loss in this range and the maximum weight loss temperature are 39.7% and 348.2°C, and the final decomposition temperature was about 450°C. After 450°C, the thermogravimetry curve tends to be stable, no weight loss occurs, and the final residual weight was approximately 35.2%.

By comparing Fig. 3b, the thermal decomposition temperature of CCS is 294.1°C, and the thermal decomposition temperature of CCSPAM is 348.2°C, indicating that the thermal stability of CCSPAM is better than that of CCS. The residual weight of CCSPAM is 35.2%, while the residual weight of CCS is 52.8%. This may be because the grafted AM monomer improves degradation rate. It can be shown that the thermal stability of the product after grafting AM on CCS is significantly better than that of CCS, and it is stable at room temperature during the application process.

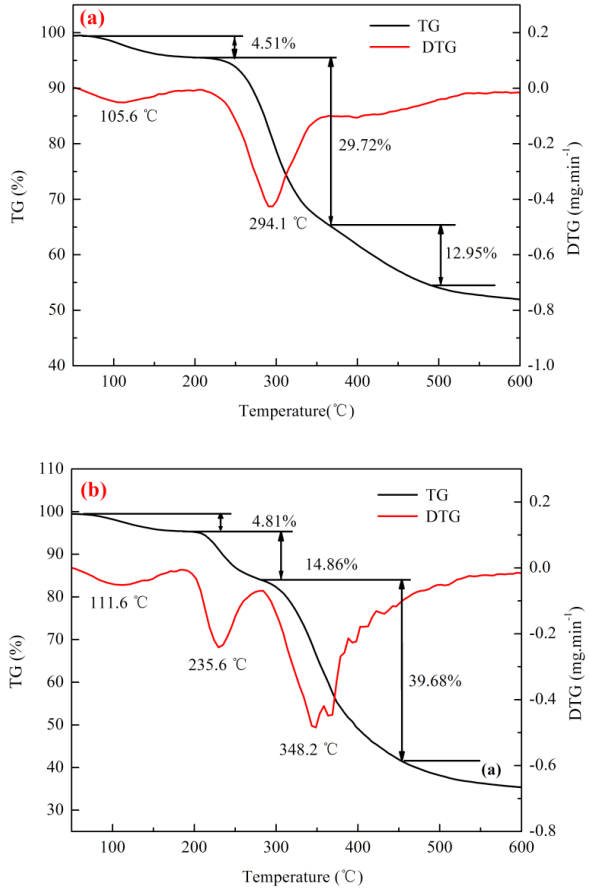

Fig. 3. TG-DTG curves: (a) CCS and (b) CCSPAM.

Table 1
The thermal gravimetric parameters of CCS and CCSPAM

Weight loss stage	Parameter	CCS	CCSPAM
First stage	Temperature range (°C)	40–200	40–200
	Weight loss (%)	4.5	4.8
	Maximum weight loss temperature (°C)	105.6	111.6
Second stage	Temperature range (°C)	200–350	200–300
	Weight loss (%)	29.7	14.9
	Maximum weight loss temperature (°C)	294.1	215.6
Third stage	Temperature range (°C)	350–500	300–450
	Weight loss (%)	13.0	39.7
	Maximum weight loss temperature (°C)	–	348.2
Fourth stage	Temperature range (°C)	–	450–600
	Residue (%)	–	35.2

3.2.5. ^{1}H-NMR spectrum

^{1}H-NMR spectrums of (a) CCS and (b) CCSPAM are shown in Fig. 4. It can be seen from Fig. 4a that the resonance peak at 3.68 ppm is assigned to the proton in the carboxyl group of the carboxylated chitosan and the resonance peak at 2.46 ppm and 2.16 ppm are attributed to the protons in the acetyl group (CH_3CO-). As shown in ^{1}H-NMR spectrum of CCSPAM, the resonance peak at 3.68 ppm is assigned to the proton in the carboxyl group, the resonance peak at 2.27 ppm corresponds to the proton of the last methyl group (-CH_2-CH-$CONH_2$) in AM, and the chemical shifts at 1.17 ppm~ 1.81 ppm correspond to the proton of methylene (-CH_2-CH-$CONH_2$) in AM. However, the chemical shift at 4.81 ppm in Figs. 4a and b are attributed to the proton of solvent, heavy water D_2O [37]. Comparing the NMR spectra before and after the modification of CCS by graft copolymerization, it is found that the proton peaks of characteristic groups AM and CCS are observed in spectrum ^{1}H-NMR spectrum of CCSPAM, indicating that the monomer successfully grafted to form CCSPAM.

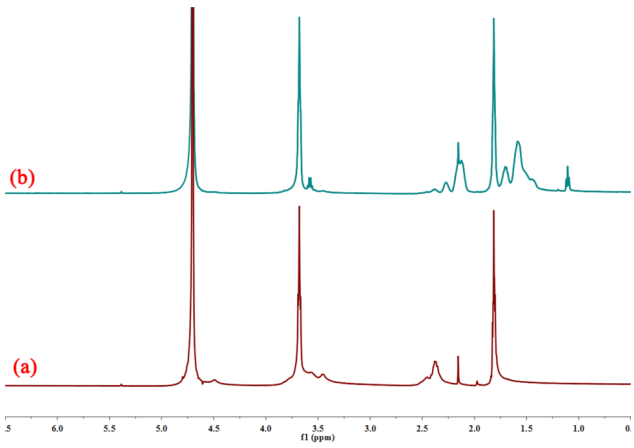

Fig. 4. ^{1}H-NMR spectrums: (a) CCS and (b) CCSPAM.

3.3. Chelation and flocculation performance

3.3.1. Effect of adding the amount of flocculants on Cu and Cr removal

Effect of adding the amount of flocculants on Cu and Cr removal is shown in Fig. 5, when the dosage is changed within the range of 10~20 mg/L, The removal efficiency of Cu and Cr show a rapid increase along with the increase of flocculants dosage. The removal efficiency of Cu and Cr achieved by CCSPAM at 2.0 mg/L are 72.9% and 69.2%, respectively. When the dosage continues to increase, the removal efficiency of Cu and Cr becomes stable.

At low dosages, the numbers of functional groups for chelation are insufficient to chelate and flocculate Cu and Cr ions by CCS and CCSPAM, resulting in weak removal ability of heavy metal ions [38]. Also, adsorption and bridging function is weak at low dosage, resulting in a poor flocculation performance [39]. The removal efficiency of Cu and Cr increases rapidly as increasing CCS and CCSPAM dosage because of the increase of chelating functional groups and adsorption sites of CCS and CCSPAM which can chelate and adsorb the Cu and Cr ions [40]. And with the continuous increase of CCS and CCSPAM dosage, the collision between flocculants, formed tinny aggregates, Cu and Cr ions are enhanced, which is conducive to bridging, thereby increasing the particle size of the flocs and accelerating settlement [41,42]. In summary, the optimal dosage for CCS and CCSPAM to remove Cu and Cr ions is 2.0 mg/L.

3.3.2. Effect of pH on Cu and Cr removal

As shown in Fig. 6, the removal efficiency of Cu and Cr by CCS and CCSPAM shows a tendency to increase first and then slight decrease with an increase in pH value and reaches an optimum Cu and Cr removal efficiency of 74.9% and 70% at pH 10 and 5, respectively. At the same time, when the pH value changes in the range of 2 ~ 4, the reduction rate of Cu and Cr ions by CCS and CCSPAM increases rapidly. But the reduction rate of Cu and Cr ions decreases slightly as the pH value continues to increase to more than 6. The optimal removal efficiency by CCSPAM of Cu^{2+} is 74.9% at pH 10.

The ability of flocculants to chelate and trap heavy metal ions in wastewater is influenced by the pH value of the reaction system. This result can be explained as follows. The ionization of –COOH groups on CCS and CCSPAM chains increase with the increase of pH value, which is beneficial to chelation and chelation and precipitation of –COOH with Cu [43]. Further, the amine groups of CCS and CCSPAM also have the function of chelating heavy metal ions. Thus, the deprotonation of amine groups increases with increasing the pH value of raw wastewater, resulting in growing adsorption for Cu^{2+} by CCS and CCSPAM [40]. Also, the copper ions can react with hydroxyl ion to form the copper hydroxide precipitate in alkaline condition. According to Fig. S8, the concentration of $Cu(OH)_2(s)$ begins to increase at pH 10–12. While the concentration of Cu^{2+} begins to decrease at pH 10–12. When pH value is more than 10, the copper ions can react with hydroxyl ion to form the copper hydroxide precipitate, and can also be chelated and flocculated by CCSPAM. So the removal of Cu^{2+} on CCSPAM rapidly increased at pH 10. Therefore, pH 6 of raw wastewater is selected as the optimal value.

3.3.3. Effect of reaction time on Cu and Cr removal

Effect of reaction time on the copper removal is shown in Fig. 7 when the reaction time varies from 0.5 to 2.0 h, the removal rate of Cu and Cr shows a steady growth trend with the increase of reaction time. The Cu and Cr removal efficiency by CCSPAM at reaction time 2.0 h are 74.8% and 70.6%, respectively. With the prolonged reaction time, the chelating and capturing capability of Cu and Cr by CCSPAM keeps stable.

Cu and Cr removal rate increase with contact time at the initial stage, Cu and Cr removal rate decreases and finally reach a stable trend. The carboxyl and amino groups of CCS and CCSPAM can chelate with Cu and Cr ions effectively at the initial stage, leading to an acceleration of chelation and flocculation and the reduction of Cu and Cr ions. But these carboxyl and amino groups of CCS and CCSPAM exhaust and thus Cu and Cr removal rate reduces with the reaction

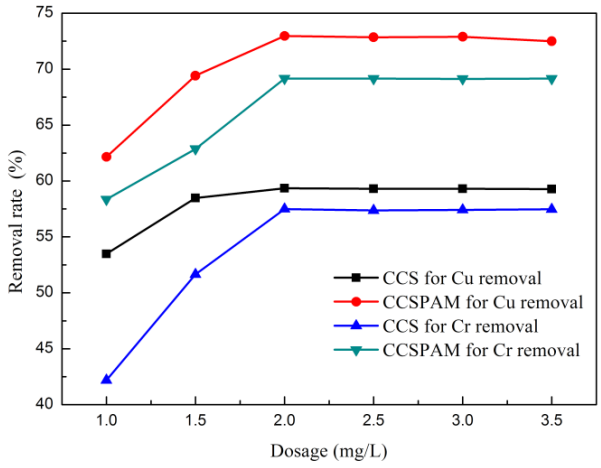

Fig. 5. Effect of adding the amount of flocculants on Cu and Cr removal.

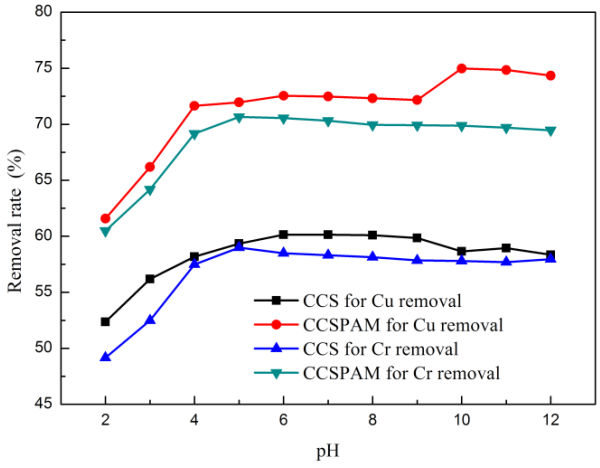

Fig. 6. Effect of pH on Cu and Cr removal.

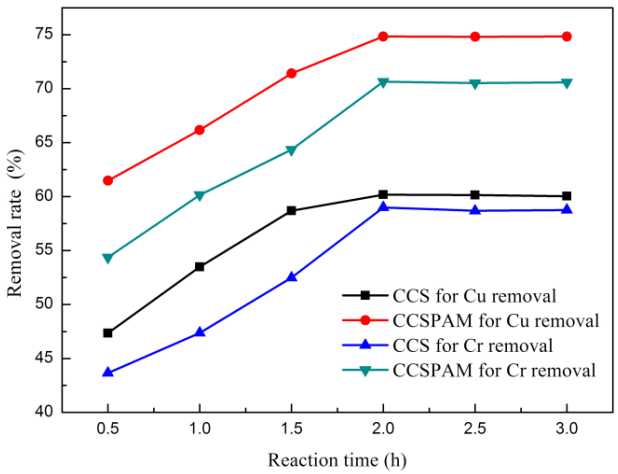

Fig. 7. Effect of reaction time on Cu and Cr removal.

time increases. Further, the remaining carboxyl and amino groups of CCS and CCSPAM become challenging to be chelated after 2.0 h of reaction time because of charge repulsion between Cu and Cr ion and flocs formed by CCS and CCSPAM in water [44]. Therefore, the optimal reaction time is 2.0 h.

4. Conclusion

In this paper, carboxylated chitosan (CCS) and acrylamide (AM) as raw materials are employed to prepare CCSPAM by UV-induced polymerization for copper removal. SEM, XRD, FTIR, and ^{1}H NMR are used to characterize the surface morphology, crystal phase, and characteristic groups of CCSPAM, and the results show that the monomers are successfully grafted to form CCSPAM with excellent thermal stability at room temperature. The effects of total monomer concentration, monomer mass ratio of CCS and AM, pH value, photoinitiator concentration, and illumination time on the synthesis performance of CCSPAM are investigated with IV, GR, and GE as indicators. The results show that the optimal condition for preparing CCSPAM are as follows: total monomer concentration 30%, monomer mass ratio 1:4, pH 7.0, photoinitiator concentration 0.03%, and irradiation time 2 h. IV, GR, and GE of the synthesized product are 1412.2 mL/g, 394.1%, and 84.1%, respectively. The flocculation results show that the optimal removal rate of Cu and Cr by CCSPAM at CCSPAM dosage 2.0 mg/L and reaction time 2.0 h is 74.8% and 70.6%, respectively. This study shows that graft copolymerization is an effective method to design naturally modified flocculants and improve the flocculation performance of natural macromolecular materials. The naturally modified flocculants have good application prospects in heavy metal treatment.

Acknowledgements

This research was supported by National Natural Science Foundation of China (No. 51508268), National Key Research and Development Program of China (2017YFB0602500), and 2018 Six Talent Peaks Project of Jiangsu Province (JNHB-038).

References

[1] H. Sone, B. Fugetsu, S. Tanaka, Selective elimination of lead(II) ions by alginate/polyurethane composite foams, J. Hazard. Mater., 162 (2009) 423–429.
[2] G. Chen, K.J. Shah, L. Shi, P. Chiang, Removal of Cd(II) and Pb(II) ions from aqueous solutions by synthetic mineral adsorbent: Performance and mechanisms, Appl. Surf. Sci., 409 (2017) 296–305.
[3] M.A. Alam, C. Wan, X. Zhao, L. Chen, J. Chang, F. Bai, Enhanced removal of Zn^{2+} or Cd^{2+} by the flocculating Chlorella vulgaris JSC-7, J. Hazard. Mater., 289 (2015) 38–45.
[4] N. Bakhtiari, S. Azizian, S.M. Alshehri, N.L. Torad, V. Malgras, Y. Yamauchi, Study on adsorption of copper ion from aqueous solution by MOF-derived nanoporous carbon, Micropor. Mesopor. Mater., 217 (2015) 173–177.
[5] T. Dong, L. Yang, M. Zhu, Z. Liu, X. Sun, J. Yu, H. Liu, Removal of cadmium(II) from wastewater with gas-assisted magnetic separation, Chem. Eng. J., 280 (2015) 426–432.
[6] X. Zhang, L. Yang, Y. Li, H. Li, W. Wang, B. Ye, Impacts of lead/zinc mining and smelting on the environment and human health in China, Environ. Monit. Assess., 184 (2012) 2261–2273.
[7] Z. Tian, L. Zhang, G. Shi, X. Sang, C. Ni, The synthesis of modified alginate flocculants and their properties for removing heavy metal ions of wastewater, J. Appl. Polym. Sci., 135 (2018).
[8] M. Ajmal, R. Rao, R. Ahmad, J. Ahmad, L. Rao, Removal and recovery of heavy metals from electroplating wastewater by using Kyanite as an adsorbent, J. Hazard. Mater., 87 (2001) 127–137.
[9] L. You, L. Song, F. Lu, Q. Zhang, Fabrication of a copolymer flocculant and application for Cr(VI) removal, Polym. Eng. Sci., 56 (2016) 1213–1220.
[10] S. Chiarle, M. Ratto, M. Rovatti, Mercury removal from water by ion exchange resins adsorption, Water Res., 34 (2000) 2971–2978.
[11] M.A. Barakat, New trends in removing heavy metals from industrial wastewater, Arab J. Chem., 4 (2011) 361–377.
[12] T. Hajeeth, P.N. Sudha, K. Vijayalakshmi, T. Gomathi, Sorption studies on Cr(VI) removal from aqueous solution using cellulose grafted with acrylonitrile monomer, Int. J. Biol. Macromol., 66 (2014) 295–301.
[13] G. Chen, C. Qiao, Y. Wang, J. Yao, Synthesis of magnetic gelatin and its adsorption property for Cr(VI), Ind. Eng. Chem. Res., 53 (2014) 15576–15581.
[14] F. Fu, Q. Wang, Removal of heavy metal ions from wastewaters: A review, J. Environ. Manage., 92 (2011) 407–418.
[15] S.K. Papageorgiou, F.K. Katsaros, E.P. Kouvelos, N.K. Kanellopoulos, Prediction of binary adsorption isotherms of Cu^{2+}, Cd^{2+} and Pb^{2+} on calcium alginate beads from single adsorption data, J. Hazard. Mater., 162 (2009) 1347–1354.
[16] S.B. Seo, T. Kajiuchi, D.I. Kim, S.H. Lee, H.K. Kim, Preparation of water soluble chitosan blendmers and their application to removal of heavy metal ions from wastewater, Macromol. Res., 10 (2002) 103–107.
[17] Z. Tian, L. Zhang, C. Ni, Preparation of modified alginate nanoflocculant and adsorbing properties for Pb^{2+} in wastewater, Russ. J. Appl. Chem., 90 (2017) 641–647.
[18] W. Ngah, K.H. Liang, Adsorption of gold(III) ions onto chitosan and N-carboxymethyl chitosan: Equilibrium studies, Ind. Eng. Chem. Res., 38 (1999) 1411–1414.
[19] Z.S. Pour, M. Ghaemy, Removal of dyes and heavy metal ions from water by magnetic hydrogel beads based on poly(vinyl alcohol)/carboxymethyl starch-g-poly(vinyl imidazole), Rsc Adv., 5 (2015) 64106–64118.
[20] K.M. You, Y.K. Park, Cd^{2+} removal by Azomonas agilis PY101, a cadmium accumulating strain in continuous aerobic culture, Biotechnol. Lett., 20 (1998) 1157–1159.

[21] D.K. Balta, N. Arsu, Y. Yagci, A.K. Sundaresan, S. Jockusch, N.J. Turro, Mechanism of photoinitiated free radical polymerization by thioxanthone-anthracene in the presence of air, Macromolecules, 44 (2011) 2531–2535.
[22] S. Sinha, S. Mishra, G. Sen, Microwave initiated synthesis of polyacrylamide grafted casein (CAS-g-PAM)-Its application as a flocculant, Int. J. Biol. Macromol., 60 (2013) 141–147.
[23] Y. Wu, N. Zhang, Aqueous photo-polymerization of cationic polyacrylamide with hybrid photo-initiators, J. Polym. Res., 16 (2009) 647–653.
[24] S.J. Lu, R.X. Liu, X.M. Sun, A study on the synthesis and application of an inverse emulsion of amphoteric polyacrylamide as a retention aid in papermaking, J. Appl. Polym. Sci., 84 (2002) 343–350.
[25] Y. Bao, J. Ma, N. Li, Synthesis and swelling behaviors of sodium carboxymethyl cellulose-g-poly(AA-co-AM-co-AMPS)/MMT superabsorbent hydrogel, Carbohyd. Polym., 84 (2011) 76–82.
[26] Y. Liao, H. Zheng, L. Qian, Y. Sun, L. Dai, W. Xue, UV-initiated polymerization of hydrophobically associating cationic polyacrylamide modified by a surface-active monomer: A comparative study of synthesis, characterization, and sludge dewatering performance, Ind. Eng. Chem. Res., 53 (2014) 11193–11203.
[27] L.Y. Liu, W.T. Yang, Inverse emulsion polymerization of acrylamide initiated by UV radiation, Acta Polym. Sin., (2004) 545–550.
[28] Y. Sun, C. Zhu, Y. Xu, H. Zheng, X. Xiao, G. Zhu, M. Ren, Comparison of initiation methods in the structure of CPAM and sludge flocs properties, J. Appl. Polym. Sci., 133 (2016).
[29] X. Li, H. Zheng, B. Gao, C. Zhao, Y. Sun, UV-initiated polymerization of acid-and alkali-resistant cationic flocculant P(AM-MAPTAC): Synthesis, characterization, and application in sludge dewatering, Sep. Purif. Technol., 187 (2017) 244–254.
[30] S.A. Seabrook, R.G. Gilbert, Photo-initiated polymerization of acrylamide in water, Polymer, 48 (2007) 4733–4741.
[31] L. Liu, J. Wu, Y. Ling, X. Li, R. Zeng, Synthesis of a novel amphoteric chelating polymer flocculant and its performance in Cu^{2+} removal, J. Appl. Polym. Sci., 127 (2013) 2082–2094.
[32] X. Yang, L. Ni, Synthesis of hybrid hydrogel of poly(AM co DADMAC)/silica sol and removal of methyl orange from aqueous solutions, Chem. Eng. J., 209 (2012) 194–200.
[33] S. Bharti, S. Mishra, Synthesis, characterization and application of polymethyl methacrylate grafted oatmeal: a potential flocculant for wastewater treatment, Int J. Environ. Res., 10 (2016) 169–178.
[34] C. Zhang, M. Zhang, Q. Chang, Preparation of mercaptoacetyl chitosan and its removal performance of copper ion and turbidity, Desal. Water Treat., 53 (2015) 1909–1916.
[35] D. Wang, T. Zhao, L. Yan, Z. Mi, Q. Gu, Y. Zhang, Synthesis, characterization and evaluation of dewatering properties of chitosan-grafting DMDAAC flocculants, Int. J. Biol. Macromol., 92 (2016) 761–768.
[36] X. Wan, Y. Li, X. Wang, S. Chen, X. Gu, Synthesis of cationic guar gum-graft-polyacrylamide at low temperature and its flocculating properties, Eur. Polym. J., 43 (2007) 3655–3661.
[37] G. Zhu, Y. Wang, W. Zhu, K. Zhu, X. Xu, Z. Shen, Facile synthesis and micellization of biodegradable poly(decamethylene succinate)-graft-poly(ethylene glycol), J. Appl. Polym. Sci., 128 (2013) 2817–2822.
[38] L. Wu, X. Zhang, L. Chen, H. Zhang, C. Li, Y. Lv, Y. Xu, X. Jia, Y. Shi, X. Guo, Amphoteric starch derivatives as reusable flocculant for heavy-metal removal, RSC Adv., 8 (2018) 1274–1280.
[39] Z. Yang, H. Yang, Z. Jiang, T. Cai, H. Li, H. Li, A. Li, R. Cheng, Flocculation of both anionic and cationic dyes in aqueous solutions by the amphoteric grafting flocculant carboxymethyl chitosan-graft-polyacrylamide, J. Hazard. Mater., 254 (2013) 36–45.
[40] C. Mahamadi, T. Nharingo, Competitive adsorption of Pb^{2+}, Cd^{2+} and Zn^{2+} ions onto Eichhornia crassipes in binary and ternary systems, Bioresource Technol., 101 (2010) 859–864.
[41] Q. Lin, H. Peng, Q. Lin, G. Yin, Formation, breakage and re-formation of flocs formed by cationic starch, Water Sci. Technol., 68 (2013) 1352–1358.
[42] T. Zhang, M. Wang, W. Yang, Z. Yang, Y. Wang, Z. Gu, Synergistic removal of copper(II) and tetracycline from water using an environmentally friendly chitosan-based flocculant, Ind. Eng. Chem. Res., 53 (2014) 14913–14920.
[43] Q. Chang, M. Zhang, J. Wang, Removal of Cu^{2+} and turbidity from wastewater by mercaptoacetyl chitosan, J. Hazard. Mater., 169 (2009) 621–625.
[44] J. Maity, S.K. Ray, Chitosan based nano composite adsorbent-synthesis, characterization and application for adsorption of binary mixtures of Pb(II) and Cd(II) from water, Carbohyd. Polym., 182 (2018) 159–171.

Supporting materials

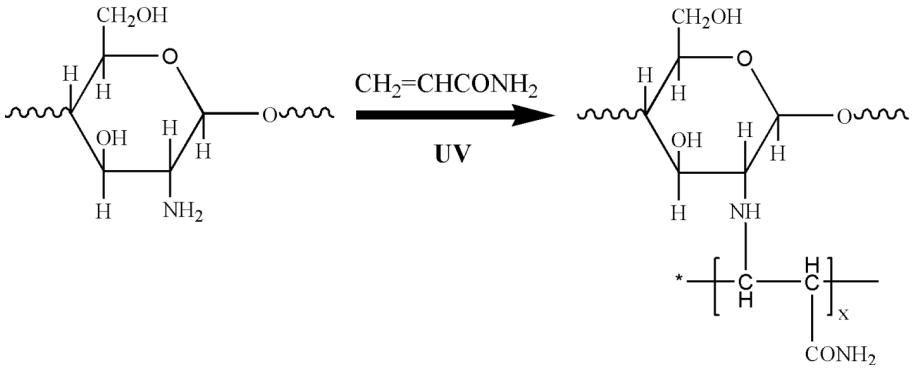

Fig. S1. Possible scheme of synthesizing CCSPAM.

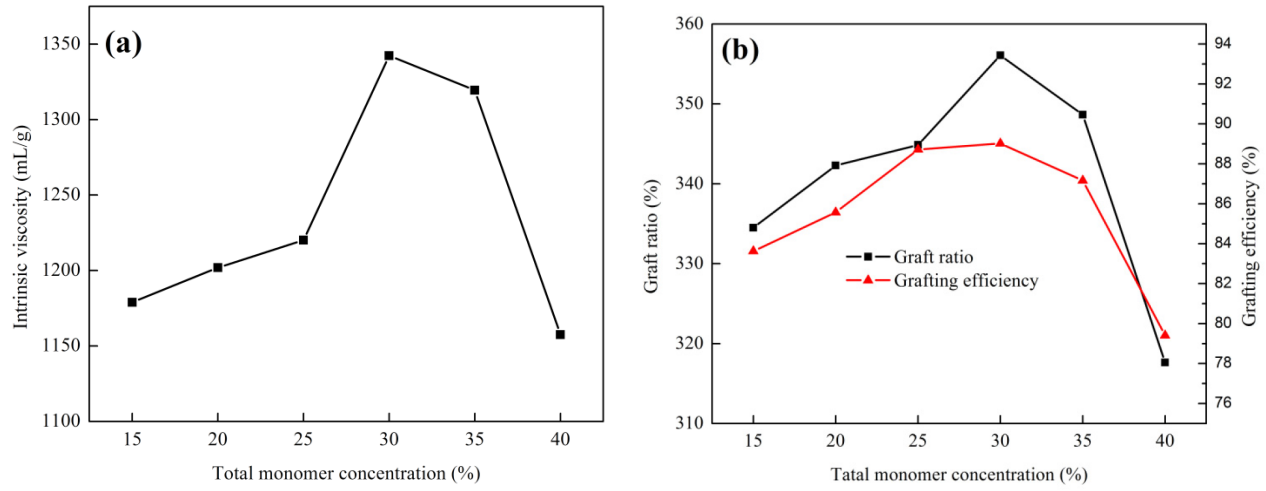

Fig. S2. Effect of total monomer concentration on (a) intrinsic viscosity and (b) grafting ratio and grafting efficiency.

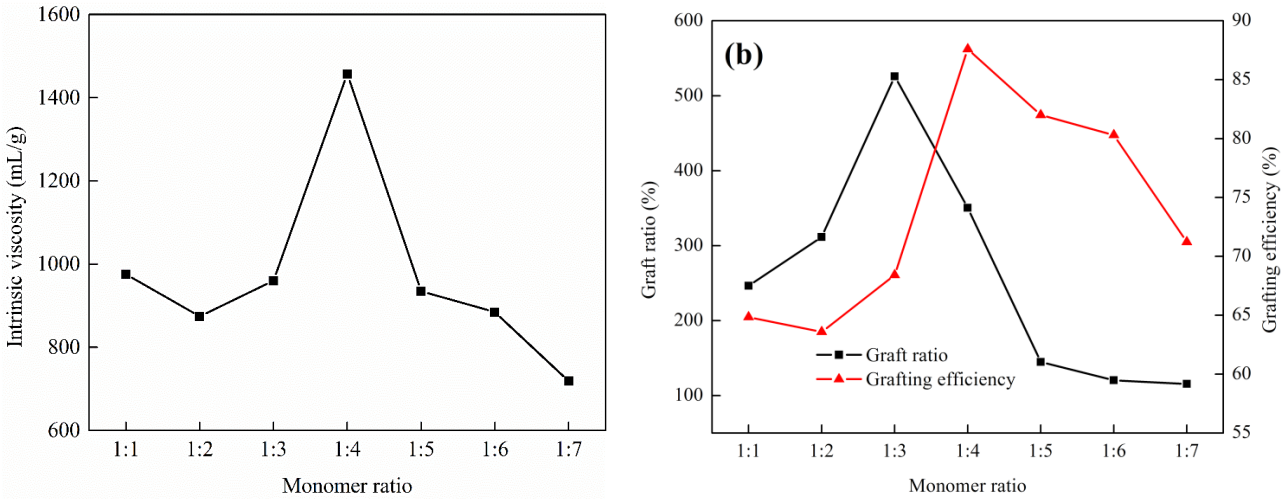

Fig. S3. Effect of monomer ratio of CCS and AM on (a) intrinsic viscosity and (b) graft ratio and grafting efficiency.

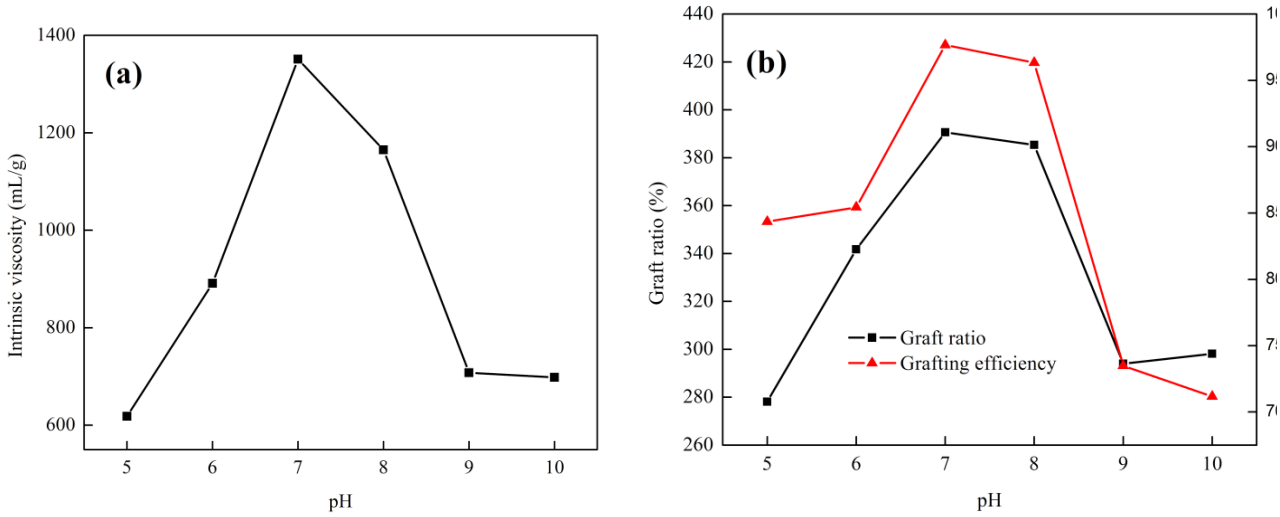

Fig. S4. Effect of pH on (a) intrinsic viscosity and (b) graft ratio and grafting efficiency.

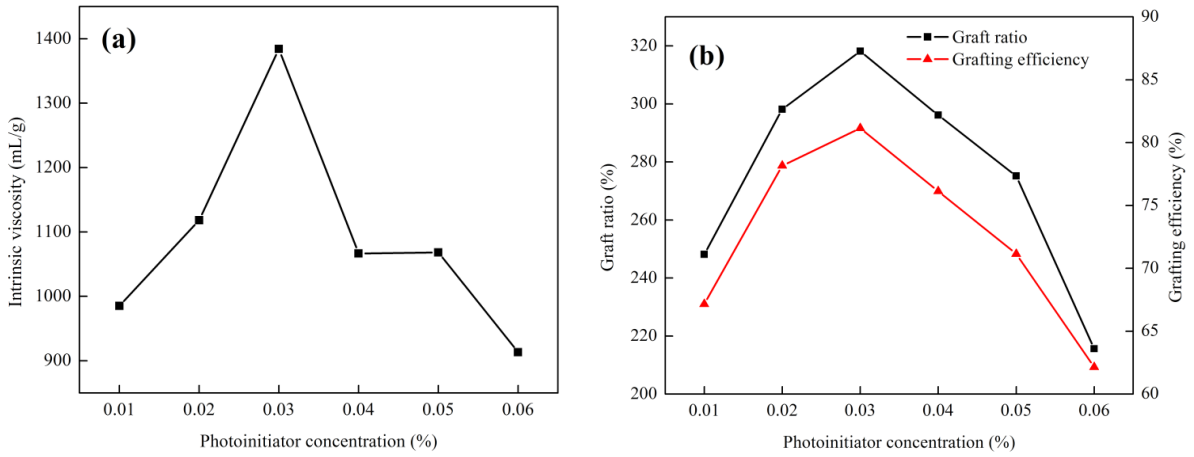

Fig. S5. Effect of photoinitiator concentration on (a) intrinsic viscosity and (b) graft ratio and grafting efficiency.

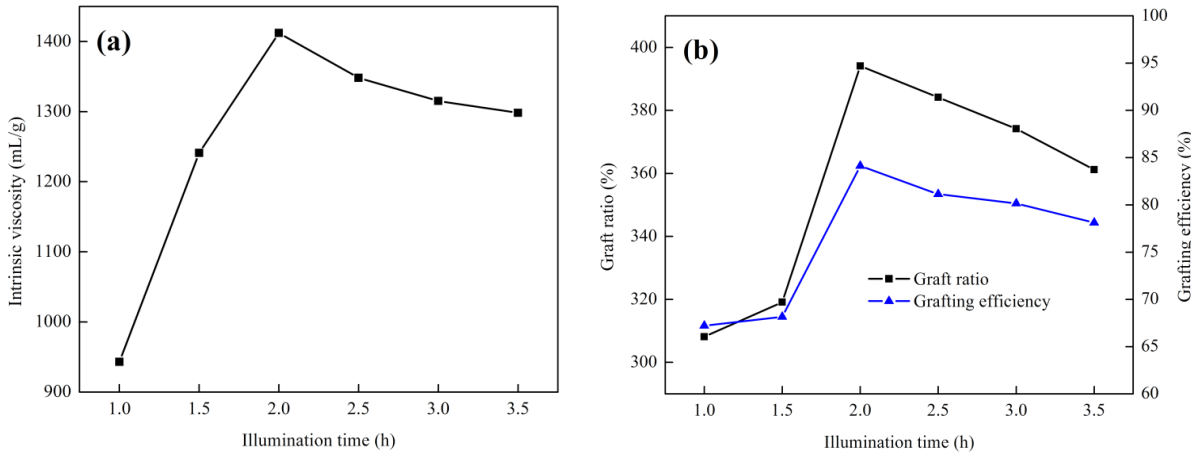

Fig. S6. Effect of illumination time on (a) intrinsic viscosity and (b) graft ratio and grafting efficiency.

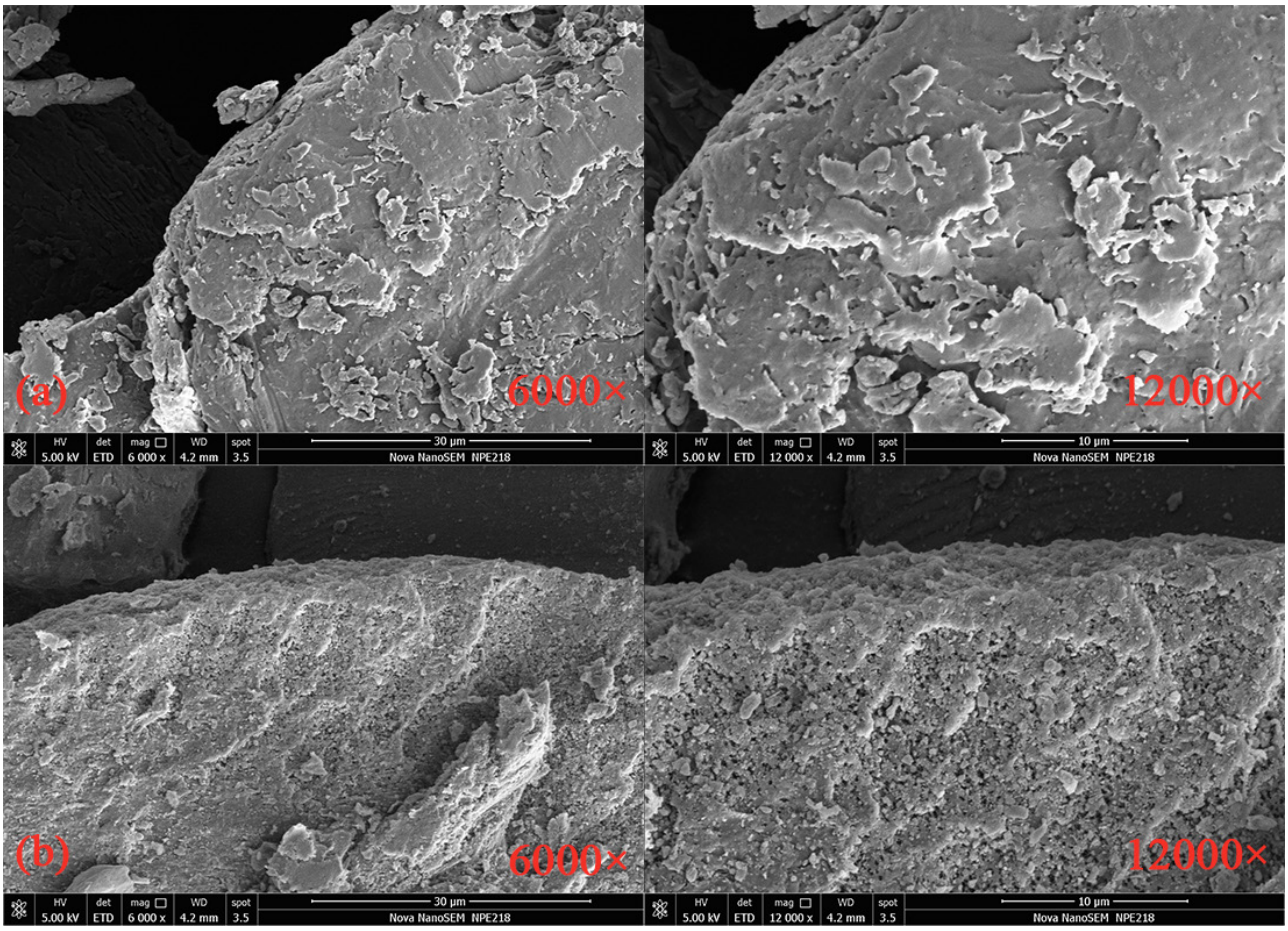

Fig. S7. SEM images: (a) CPCTS and (b) CCSPAM.

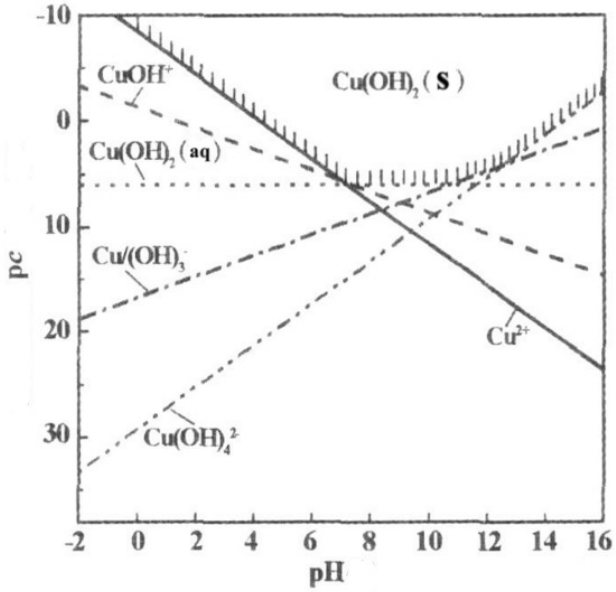

Fig. S8. Diagram of pc-pH of Cu^{2+}-H_2O system at 298.15K. (*T.W.J. Albrecht, J. Addai-Mensah, D. Fornasiero, Effect of pH, Concentration and Temperature on Copper and Zinc Hydroxide Formation/Precipitation in Solution, Chemeca 2011: Engineering a Better World: Sydney Hilton Hotel, NSW, Australia, 2011. 2100.; H. Chang, L. Chai, Y. Wang, Y. Shu, M. Zhou, Study on equilibrium of hydroxyl complex ions in Cu^{2+}-H_2O system, Min. Metal. Eng., 6 (2007) 37–40. (In Chinese)).*